Statistically enhanced classification of centrifugal compressor operating condition

Statistically enhanced classification of centrifugal compressor operating condition

M. Stajuda [1], **D. García Cava** [1], **G. Liśkiewicz** [2]
[1] Institute for Infrastructure and Environment, School of Engineering, University of Edinburgh, Edinburgh, United Kingdom

[2] Institute of Turbomachinery, Lodz University of Technology, Lodz, Poland
e-mail: **mateusz.stajuda@ed.ac.uk**

Abstract

Centrifugal compressors operating near peak efficiency are prone to aerodynamic instabilities, which in extreme cases, may lead to quick destruction of the machine. Instabilities are flow structure of different character, which are not straightforward to detect. One of the possible approaches could take advantage of feature space representation. Historic data might be used for building clusters of operating conditions and defining class boundaries. Then, a new point could be classified based on its location in feature space relative to those boundaries. Different instabilities can coexist temporarily when transitioning from conditions to another, which makes defining the boundaries in the transition zones a challenge. To deal with those problems, an application of Gaussian Process Classification (GPC) method is proposed. Being a non-parametric method of high flexibility, it can provide better separation between conditions in the feature space. GPC output provides a confidence level of a new observation belonging to a class, which can be used for classification but also to introduce a no-classification zones based on class probability values, which could decrease the error rate in transition zones. In this study, GPC is applied to classify features obtained from physically interpretable feature extraction method for a centrifugal compressor. Three different classes are defined, one stable and two related to different instabilities. The classification with GPC is compared to threshold approach, based on physical interpretation of the features. The results demonstrate that GPC offers a more flexible and data-driven separation of classes, especially in transition zone between different flow conditions, however the rejection zone does not prove to provide improvement in the analysed case. Compared to the threshold approach, GPC requires historic data for all conditions and results depend strongly on data labels. If the physical interpretation of the features is possible, the advantages of GPC in the transition zone can be combined with the binary threshold approach in well-defined feature space regions.

1 Introduction

Detection of aerodynamic instabilities is an important issue to ensure safety and efficiency of compressor operation [1]. The general term instabilities encompasses a number of different phenomena, such as inlet recirculation [2], rotating stall [3] or surge [4] that negatively influence the performance and can lead to the destruction of the machine. The impact of instabilities varies depending on the type of phenomenon occurring, design of the machine and operating conditions [4]. In some cases, milder instabilities such as inlet recirculation or rotating stall can be used as an early indication of the ultimate instability - surge, in different cases surge is not preceded by any other instability. However, the presence and order of instabilities appearance with increasing throttling depends on many aspects, including the rotational speed of the impeller [5]. Therefore, it is the most desired to understand the operating conditions at each instant of the compressor operation. Such indication should be robust to avoid false alarms and quickly to enable prompt reaction in case of appearance of the instabilities.

Detection of instabilities was shown to be possible using data-driven techniques, by analysing the frequency

spectrum [6] or energy of specific frequency bands [3]. Recently, the application of different decomposition techniques was demonstrated to be applicable for understanding the operating conditions of a compressor including empirical mode decomposition (EMD) [7, 8] and singular spectrum analysis (SSA) [9, 10]. With both methods, the signal is decomposed into a number of components, some of which can be used to highlight the changes in the signal resulting from the presence of instabilities. The components are time series that need to be furtherly processed to obtain an instability sensitive feature. Features can be built by taking advantage of energy, frequency or other parameters of the components [11]. Depending on the decomposition algorithm, the features can be interpretable or abstract, with the former meaning that the connection between the features and the system physics is fully traceable. The data can be represented in so-called feature space to allow for interpreted classification of new data [11]. The feature space can be multivariate, with dimensionality equal to the number of features.

With a recent study, a framework based on compressor operating conditions mapping to feature space was proposed [12]. It was demonstrated that using EMD on a pressure signal from different locations inside of the compressor, the features based on energy of selected components could be used for representing different operating conditions. The approach proved to be very sensitive, allowing for robust and quick detection of inlet recirculation and surge. An observed shortcoming was an early reaction of the system to initial surge symptoms, leading to early surge detection, which might unnecessarily limit the operating range of the compressor. To deal with this problem, an approach based on supervised classification was proposed. Advanced classifiers allow for great flexibility of the boundaries between classes, ensuring optimal classification with respect to the training data labels. Some of the classifiers can provide not only class assignment but also a measure of certainty of the point belonging to a class. This information can offer additional benefits, as a reject option can be formulated [13]. It could be beneficial in locations of feature space where probability of neither of the classes is high. Introduction of rejection option can offer a decrease in error rate, which in case of compressor analysis could be false indication of surge .

One of the advanced classifiers with probabilistic output is Gaussian process classifier (GPC). GPC is a non-parametric algorithm that can be applied to binary as well as multiclass classification problems [13]. A Gaussian process is a collection of random variables, any finite number of which have a joint Gaussian distribution. Taking advantage of this formulation of the problem, it is possible to infer the class of a new point based on previous observations of values of features for this new point. Using GPC, the level of probability of belonging to selected class can be found for each location in the feature space. Thus, knowing a location of a query point, the probability of that point belonging to a class can be obtained. Due to high flexibility of the GPC algorithm, the shape of probability contours defining boundaries between classes is strongly data-driven and can be optimized to best represent the data [13]. The aim of this study is to investigate the application of Gaussian process classification for statistically-enhanced detection of centrifugal compressor operating conditions.

The study is organized as follows. First, methodology regarding feature extraction and classification with GPC and threshold approach is given. The test rig for a compressor used for validation of the methodology is described. Then, the results of GPC method application are demonstrated and the outcomes are compared with threshold approach. The improvement due to GPC is quantified, and influence of the rejection zone introduction is discussed. Finally, the limitations and challenges of GPC are discussed and potential recommendations for the application in a monitoring system are given.

2 Methodology

2.1 Feature space representation and class boundaries

The feature space representation in this study is constructed using components obtained with empirical mode decomposition (EMD). The features are representative for the energy of flow fluctuations at different scales. EMD is an algorithm that iteratively extracts subsequent modes of oscillations from the signal. Those modes, called intrinsic mode functions (IMFs), are amplitude and frequency modulated time series of a length equal to the input signal. A detailed description of EMD algorithm can be found in [14].

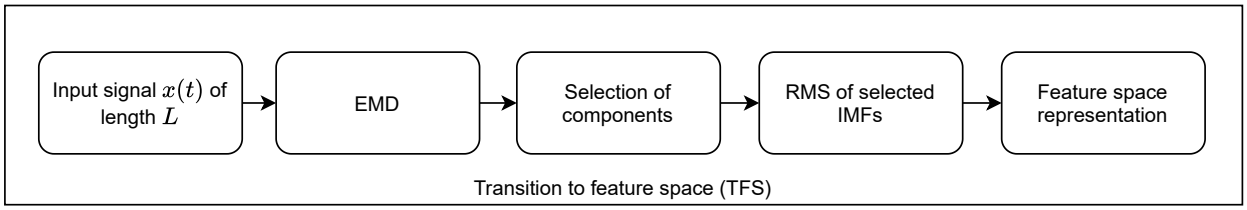

Figure 1: Transformation of input signal to a feature space representation

The procedure to obtain feature space representation from input signal is demonstrated in Figure 1. First, the static pressure signal $x(t)$ of length L is collected from selected location inside the compressor. It is then subjected to EMD to obtain a set of IMFs. Specific IMFs or groups of IMFs are selected, based on prior knowledge and experience or extended analysis [12]. To construct a feature, the root mean squared (RMS) value of the IMFs is computed. Though this procedure, the input signal of length L gets to be represented as a single value of a feature. This procedure has to be repeated for the number of times equal to the dimensionality of feature space N_F. For a single portion of data, a vector of feature values is obtained $\mathbf{x}_i = [x_1, x_2, .., x_{NF}]$. The values of features are used to map the points onto the space.

For classification of an unknown data point, the feature space is divided into classes and class boundaries are introduced. The boundaries of feature space are set based on training data. Training data points can be represented as a set $\mathbf{D} = (\mathbf{X}, \mathbf{y})$, where $\mathbf{X} = [\mathbf{x}_1, \mathbf{x}_2, ..., \mathbf{x}_N]$, $\mathbf{X}_i \in R^N$ is a matrix of N feature vectors and $\mathbf{y} = [y_1, y_2, ..., y_N]$ is a vector of classes. The classes are represented with integer values $y_i \in \{1, 2, ..., k\}$. A single class value is assigned for each feature vector representative for given portion of the signal. Having a feature vector $\mathbf{x}_*$ for a new observation, the aim is to predict its class y_*. To do so, the location of the new point in feature space has to be found, relative to the class boundaries. In this study, two different approaches to defining boundaries are compared - Gaussian process classification and thresholds based on physical interpretation of the features. The flowchart for classification methodology is shown in Figure 2.

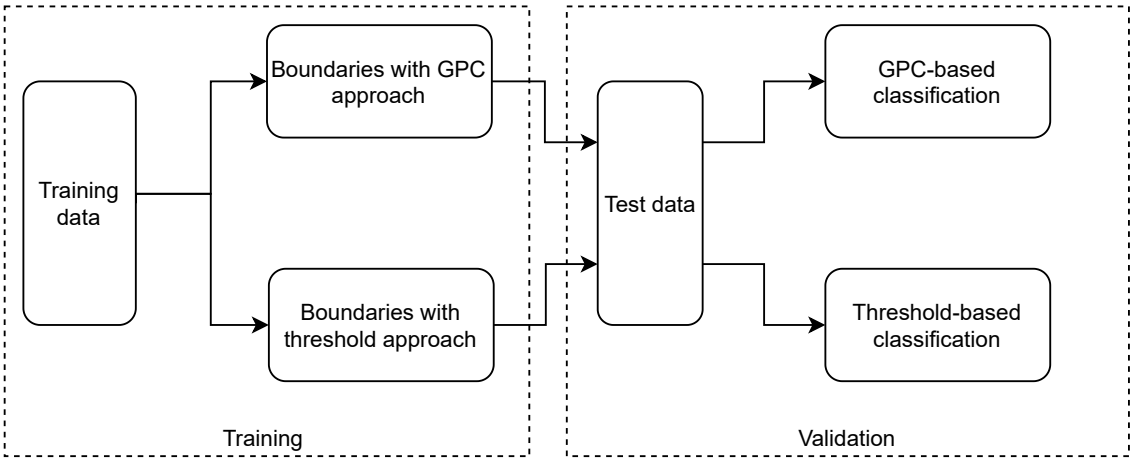

Figure 2: Flowchart of training and validation approach in the study

2.2 Gaussian process classification approach

Gaussian process classification is made using training data for all of the available classes. The class boundaries are driven by the choice of covariance function type, its parameters and training data.

Gaussian process classification is based on Gaussian process regression, bearing certain similarities to logistic regression [13]. For binary classification, a regression problem is solved with input being the features vector and target being class labels. It is subsequently translated into classification with use of a latent

function, for example logistic function [13]. The mathematical formulation of GPC is building upon the regression, thus a Gaussian process regression is introduced first. A more in-depth description of Gaussian process for classification can be found in textbooks of Rasmussen [13] or Bishop [15].

2.2.1 Gaussian process regression

A regression problem aims to find a function f that connects the input variable, or to the output variable. In majority of cases also noise term ϵ is involved, to account for the fact that taken observations (t) are bearing also a certain amount of noise. This noise can be assumed to be normally distributed. A general regression problem can be therefore described as in equation (1).

$$t = f(x) + \epsilon \tag{1}$$

A Gaussian process, by definition, is a collection of random variables, any finite number of which have a joint Gaussian distribution. Observing a process, we can obtain a dataset $\mathbf{D} = (\mathbf{X}, \mathbf{t})$, where $\mathbf{X} = [\mathbf{x}_1, \mathbf{x}_2, ..., \mathbf{x}_N]$, $\mathbf{x}_i \in R^N$ is a matrix of N feature vectors and $\mathbf{t} = [t_1, t_2, ..., t_N]$ is a vector of target values. We are representing a given physical process that lead to obtaining a $\mathbf{D}$ data set as a Gaussian process (equation (2)) for the purpose of modelling the mapping function f. A Gaussian process can be fully described by mean function $m(x)$, and covariance function $k(x, x')$, which can be defined as in equations (3) and (4) respectively, where $E[\cdot]$ stands for an expected value.

$$f(x) \sim \mathcal{GP}(m(x), k(x, x')) \tag{2}$$

$$m(x) = E[f(x)] \tag{3}$$

$$k(x, x') = E[(f(x) - m(x))(f(x') - m(x'))] \tag{4}$$

A Gaussian process uses distribution over functions, assigning probability of a given function fitting the data. For a noise-free case we can obtain values of functions for input $\mathbf{X}$ as $\mathbf{t} = [f(\mathbf{x}_1), f(\mathbf{x}_2)..., f(\mathbf{x}_n)]$. Taking advantage of Gaussian formulation, we can assume a joint distribution of the known functions values $\mathbf{t}$ and unknown values $\mathbf{t}_*$, which we try to predict based on new inputs $\mathbf{X}_*$. The joint distribution is given by equation (5). It is a common approach in practical applications to assume zero mean [13].

$$\begin{bmatrix} \mathbf{t} \\ \mathbf{t}_* \end{bmatrix} \sim \mathcal{N}\left(0, \quad \begin{bmatrix} \mathbf{K_t} & \mathbf{K}_* \\ \mathbf{K}_*^\mathbf{T} & \mathbf{K}_{**} \end{bmatrix}\right) \tag{5}$$

The covariance matrix is composed of four terms representing the relations between training data $\mathbf{X}$ and new data points vector $\mathbf{X}_*$. In this equation $\mathbf{K_t} = k(\mathbf{X}, \mathbf{X})$ is the covariance between training points, $\mathbf{K}* = k(\mathbf{X}, \mathbf{X})$ represents for the covariance of training points and new data points and $\mathbf{K}_{**} = k(\mathbf{X}_*, \mathbf{X}_*)$ represents the covariance for test data vector, therefore it is a scalar value.

The covariance can be computed as in equation (4) or obtained with so-called kernel function. The kernel function defines covariance based solely on the inputs. A commonly used kernel function, also employed in this study, is radial basis function (RBF) shown in equation (6). For this function, is expected that for two inputs located close to each other, the outputs would have a similar value. The two parameters of a kernel function, called hyperparameters are lengthscale l and variance σ. The variance defines average distance of the function away from its mean, while lengthscale influences the scale of function variability [16].

$$k(x, x') = \sigma^2 \exp\left(-\frac{d(x, x')^2}{2l^2}\right) \tag{6}$$

With all the abovementioned assumptions, having defined the prior and using test points we can infer about the posterior. The posterior is given by equation (7). It is normally distributed with mean $m(\mathbf{t}_*)$ and co-

variance $cov(\mathbf{t}_*)$, which can be computed as per equations (8) and (9) respectively. Using the outcomes of regression, the predictive distribution for new input data vector $\mathbf{X}_*$ can be

$$p(\mathbf{t}_*|\mathbf{X}_*, \mathbf{X}, \mathbf{t}) = \mathcal{N}(m(\mathbf{t}_*), cov(\mathbf{t}_*)) \tag{7}$$

$$m(\mathbf{t}_*) = \mathbf{K_t}_*^T \mathbf{K_t}^{-1} \mathbf{t} \tag{8}$$

$$cov(\mathbf{t}_*) = \mathbf{K}_{**} - \mathbf{K}_*^T \mathbf{K_t}^{-1} \mathbf{K}_* \tag{9}$$

It can be noted that the covariance does not depend on the output values $\mathbf{t}$ but only on the covariance. Due to this, the prediction of the model will strongly depend on the type of covariance function chosen and its hyperparameters. Those hyperparameters can be represented through a vector θ. To ensure the fit of functions to the data, the hyperparametrs are optimized to maximize the log marginal likelihood L, given by equation (10), with $|\mathbf{K_t}|$ being a determinant of $\mathbf{K_t}$.

$$L(\theta) = log(p(\mathbf{t}|\mathbf{X})) = -\frac{1}{2} log|\mathbf{K_t}| - \frac{1}{2}\mathbf{t}^T \mathbf{K_t}^{-1}\mathbf{t} - \frac{N}{2} log(2\pi) \tag{10}$$

2.2.2 Transformation of regression into classification

A binary classification problem requires the output to be in a range [0, 1] to be representative for a class probability. To translate the regression problem into binary classification, the regression outcome t is transformed through an additional function. A commonly used function is a logistic function as in equation (11).

$$\sigma(t) = \frac{1}{1 + exp(-t)} \tag{11}$$

In this case we are interested in finding a class for a given feature vector $\mathbf{x}_*$. With a binary classification, it is enough to predict classes for a single class $p(y_* = 1|\mathbf{x}_*, \mathbf{X}, \mathbf{t})$, as the other class probability $p(y_* = -1|\mathbf{x}_*, \mathbf{X}, \mathbf{t})$ can be deduced as $1 - p(y_* = 1|\mathbf{x}_*, \mathbf{X}, \mathbf{t})$. To obtain the predictive distribution for a class $y = 1$, the integral from equation (12) is evaluated. It is not analytically traceable, therefore it has to be approximated, for example using Laplace method [13].

$$p(y_* = 1|\mathbf{x}_*, \mathbf{X}, \mathbf{t}) = \int \sigma(t_*) p(t_*|\mathbf{x}_*, \mathbf{X}, \mathbf{t}) df_* \tag{12}$$

The binary classification can be translated into a multiclass one using one-vs-all approach [17]. A number of binary classifier is trained on differently configured data. The data for a class of interest is treated positive and data for all other classes is considered negative. This is repeated for all the classes. The probability for each classifier is then combined to ensure that the output is within the range $[0, 1]$.

The GPC algorithm applied in this study is a Python implementation included in scikit-learn library [18] based on formulation shown by Rasmussen [13]. The method is not fully multiclass, but rather uses a series of one-vs-all binary classifications to deal with a multiclass problem. Using Gaussian process approach, the kernel function has to be specified and optimized. The kernel parameters for RBF function chosen in this study are optimized with a built-in optimization procedure, using gradient-based optimizer L-BFGS-B [18]. A kernel hyperparameters vector θ is obtained for every one-vs-all binary classification. As output of GPC algorithm, the probability of a point in feature space belonging to each class is given. Considering three classes used in this study, the probabilities can be stated as p_{c1}, p_{c2}, p_{c3}. The default classification approach implemented in scikit-learn assigns the most probable class to a given query point. In parallel to the threshold method, one can consider the classification to be a check of three hypotheses, marked $\mathbf{H}_1$ to $\mathbf{H}_3$.

$$\mathbf{H}_1 : (p_{c1} > p_{c2}) \,\&\, (p_{c1} > p_{c3}) \rightarrow \text{Class 1} \tag{13a}$$
$$\mathbf{H}_2 : (p_{c2} > p_{c1}) \,\&\, (p_{c2} > p_{c3}) \rightarrow \text{Class 2} \tag{13b}$$
$$\mathbf{H}_3 : (p_{c3} > p_{c1}) \,\&\, (p_{c3} > p_{c2}) \rightarrow \text{Class 3} \tag{13c}$$

Having all the information regarding all class probabilities, it is possible to provide more sophisticated classification conditions or introduce a reject option, where no class is assigned to the data point. Apart from classification, the probability estimation can allow to investigate stability changes within a class, which is not possible with binary classification approach. The disadvantage of GPC compared to threshold approach is that the data representing all classes is needed.

2.3 Threshold approach

In the threshold approach, the boundaries between classes are constructed using a single class - Class 1. Two independent features, x_1 and x_2, are used to map the data onto two-dimensional feature space. The threshold value for the first feature is marked T_{x_1} and for second feature T_{x_2}. The thresholds are constructed using high percentile of data distribution to diminish the influence of outliers that may be present in the pressure signal. In this study 99$^{\text{th}}$ percentile of the distribution is used. For a new unknown observation to be classified, it is compared against the thresholds in a sequential manner. First, the IR feature is examined. Two hypotheses - $\mathbf{H}_4$ and $\mathbf{H}_5$ are tested, allowing to investigate if the compressor is generally stable or unstable.

$$\mathbf{H}_4 : x_1 \leq T_{x_1} \rightarrow \text{Class 1} \tag{14a}$$
$$\mathbf{H}_5 : x_1 > T_{x_1} \rightarrow \text{Class 2 or Class 3} \tag{14b}$$

If $\mathbf{H}_5$ is fulfilled, then the next set of hypotheses is investigated - $\mathbf{H}_6$ and $\mathbf{H}_7$. Depending on which of those is true, the indication of type of instability is either inlet recirculation or surge.

$$\mathbf{H}_6 : x_2 \leq T_{x_2} \rightarrow \text{Class 2} \tag{15a}$$
$$\mathbf{H}_7 : x_2 > T_{x_2} \rightarrow \text{Class 3} \tag{15b}$$

Using this indication, decision about the actions in regards to the operating machine can be made. The presence of surge would possibly lead to engaging a surge-suppressing mechanism [19]. It would disrupt normal operation of the machine, therefore it should take place as close to the true danger zone as possible in order not to limit the operating range of the compressor.

3 Experimental test rig and data collection

The measurements of static pressure used in this study were obtained from two locations inside a single-stage centrifugal compressor. Data was acquired using subminiature Kulite transducers (XC0-080 series) mounted flush to the shroud walls. The operating conditions of the compressor were changed through throttling with a valve downstream the outlet section. The level of throttling was defined as a throttle opening area (TOA) being the relation of the open flow area to restricted flow area at the valve section expressed in percent. The rotational frequency of the compressor was kept constant at 100 Hz and pressure data was sampled at 100 kHz. Figure 3 demonstrates the cross section of the compressor with indicated locations of sensors. A detailed description of the test rig can be found in [20].

The data used in this study was collected under two different protocols. The first protocol lead to obtaining a set of data termed quasi-dynamic (QD). The measurements were performed in an iterative procedure where

the throttling was changed in a step-wise manner and a set of data was collected for given constant position of a valve. A number of position was used to obtain data for different operating conditions. The other protocol lead to obtaining dynamic data (D), which was collected while the throttle position was constantly changed in the process, increasing the throttling level. The throttle positions used for obtaining the dynamic data were within the range for which quasi-dynamic data was collected. In previous study it was demonstrated that two locations inside the machine were sufficient to represent the operating conditions of the compressor [12]. The first location was before impeller, using p_{s-imp1} sensor and the other was at the outlet, using p_{s-out} sensor. For the described machine, two distinct instabilities were observed - inlet recirculation (IR) and surge.

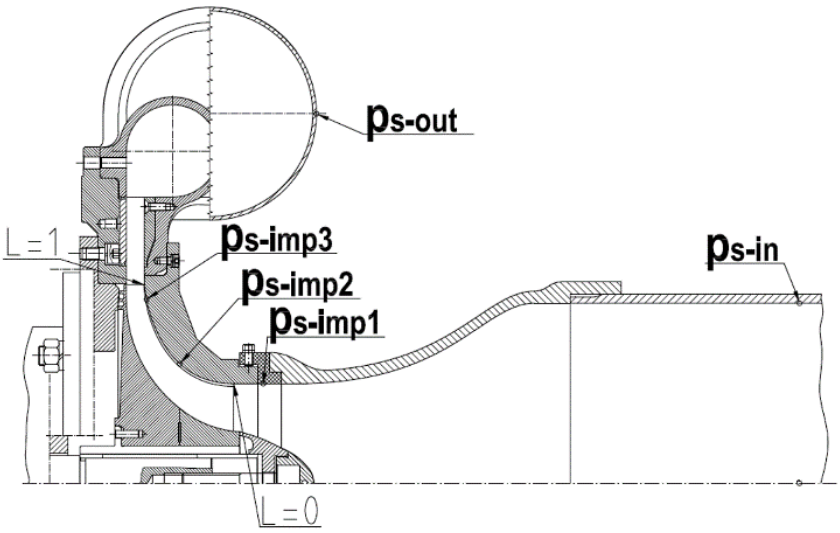

Figure 3: Cross-section of the experimental rig with pressure transducer locations [20]

The methodology presented in this study was used for the data from a centrifugal compressor. Using prior knowledge about the data [20], three classes were defined in the data. Class 1 being stable conditions, class 2 - inlet recirculation conditions and class 3 - surge conditions, making $c_i \in \{1, 2, 3\}$. Two features were used to represent the data in the feature space, x_1 and x_2. The first feature, x_1, obtained as RMS of IMF 6 from p_{s-imp1} sensor before impeller was shown to be related to inlet recirculation intensity, but it could also be used to differentiate stable and all unstable conditions. The second feature - x_2 was obtained as RMS of IMFs 9 to 11 from p_{s-out} sensor at the outlet. It is related to surge intensity and allows to differentiate between the type of instability - inlet recirculation or surge - when the unstable conditions are present. A thorough description of the feature extraction procedure, choice of features and discussion on their physics can be found in [12].

For the purpose of training and validation of the method, two data subsets are defined. The training subset is the quasi-dynamic data, obtained within a range from 35 to 8% of TOA with a step of approximately 1%. The validation set is the dynamic data, representing a dynamic transition from stable to fully unstable conditions. The count of data for training and validation in each of the classes is given in Table 1 in terms of number of points in the feature space.

Table 1: Training and validation data count

Data type	Quasi-dynamic	Dynamic
Condition	Benchmark	Validation
Stable (c_1)	280	60
Inlet recirculation (c_2)	240	30
Surge (c_3)	180	110

4 Results and discussion

The very first step in the analysis is confirmation that the mapping obtained with quasi-dynamic data can be representative for the dynamic data. It is not obvious as the data are collected under different protocols. A more abrupt change in throttling can render more dynamic behaviour of the flow, resulting in an increased level of fluctuations due to higher process dynamics. Figure 4 demonstrates the mapping of quasi-dynamic and dynamic data in the feature space. The features for stable conditions are concentrated in a confined location in feature space. The data for inlet recirculation sets off from that location and forms a path. It first moves upwards due to increase in x_1 feature value, up to the peak of inlet recirculation intensity and then gradually moves to the right with increase in x_2 feature value and downwards with decrease in x_1 feature. The points for dynamic data follow the same path and overlap the quasi-dynamic data in feature space. Therefore, quasi-dynamic data can be considered representative for the dynamic data, rendering the general approach based on mapping with use of quasi-dynamic data viable.

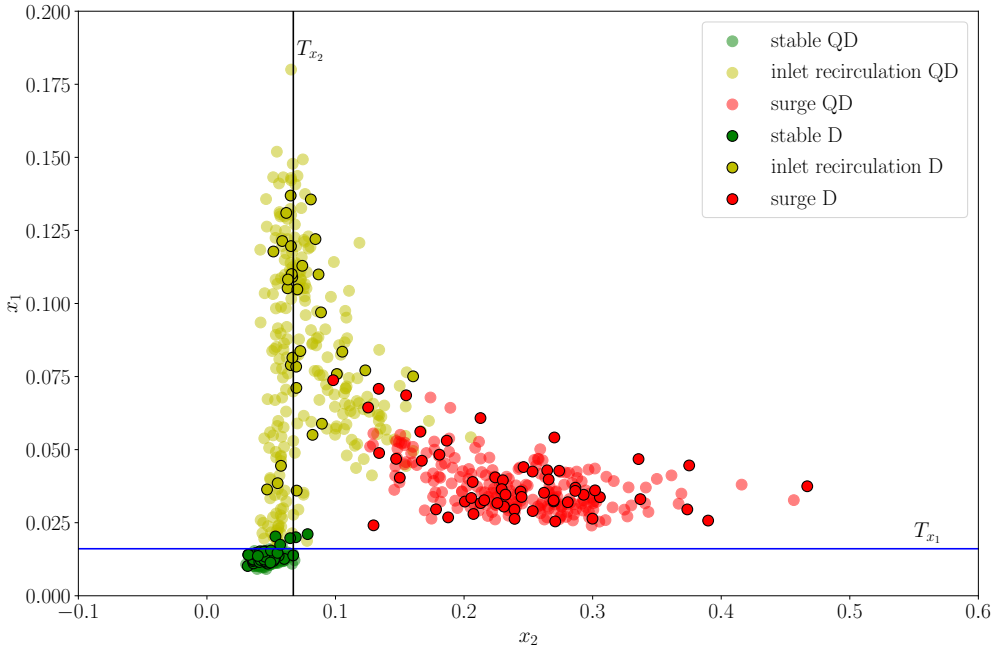

Figure 4: Mapping of the data in the feature space for quasi-dynamic and dynamic data; straight lines depict thresholds T_{x_1} (blue) allowing to separate stable and unstable conditions and T_{x_2} (black) used for differentiation of instability type

The thresholds obtained from stable conditions for both x_1 and x_2 features are also shown in Figure 4. Those threshold serve as class boundaries in the threshold approach. It can be noted that a good separation of stable from unstable conditions is provided with T_{x_1} threshold, as it represents the intensity of the first instability appearing in the system. The position of T_{x_2} threshold is representative for most of the data before the peak of inlet recirculation. After the peak, the points labelled as belonging to inlet recirculation class tend to exceed the threshold. The points for dynamic signal for IR class seem to be shifted slightly to the right compared to quasi-dynamic.

Considering T_{x_2} threshold as a decision boundary for surge detection, the instability would be detected earlier than it should. On the other hand, this formulation ensures that all of the surge points are classified correctly, which is important from safety perspective. In a surge-detection system employing the threshold approach, a surge indication would appear early, making it very conservative and possibly unnecessarily limiting the operating range of the machine.

To obtain new, data-driven boundaries, the GPC is used. A posterior probability distribution is computed using training data and the kernel function. The hyperparameters of the kernel (σ and l) are optimized to

ensure the best fit of the posterior to the training data. To visualize the posterior distribution, probability value for each class is obtained for a grid of points and plotted as a colormap in Figure 5.

Three classes present in the picture differ in both shape and size. A very concentrated stable values cluster is represented by a high-probability area (above 0.8) several times bigger than the cluster itself. For inlet recirculation, the high probability region is also big, containing most of the training points, while in case of surge the high probability region is very small compared to the extent of data. The shaping of the posterior is dependent on both training data and choice of kernel function. The optimization method aims to increase fit to the data, which doesn't have to mean that the clusters with optimal parameters are closely encompassing the data. This can be both beneficial and problematic, depending on the character and distribution of the data. The distance between iso-probability lines is the smallest in transition regions indicating sharp changes in class probability. The peak for surge class probability is located relatively close to the boundary between clusters and encloses only a small number of surge points.

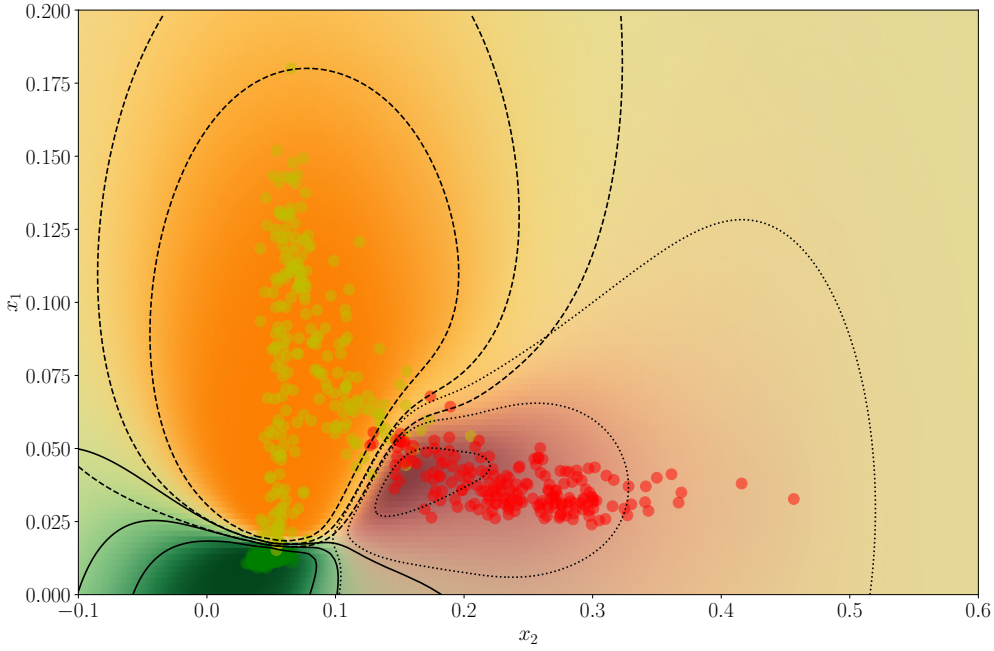

Figure 5: Probability distribution (colormap) and training dataset (scatter points); the intensity of the colors of colormap is related to probability of a class, with green for stable conditions, orange for inlet recirculation and red for surge; iso-probability lines at values 0.4, 0.6 and 0.8 plotted with different types of lines; the training dataset coloring follows the same scheme as in a previous figure

Figure 6 demonstrates the comparison between threshold method boundaries and GPC-based boundaries with the test data. Comparing the shapes of boundaries, the one between IR and surge is shifted far to the right and changed from vertical line to an inclined, but could still be quite well represented with a straight line. This means that surge is to be detected for a much higher value of x_2 that in threshold approach. With x_2 representing the energy of certain flow scales, it means that stronger structures will be allowable within the stability limit. The class boundary between stable and IR conditions remained very similar to blue threshold defined on x_1 in the proximity of training points. Further from training points, it shape was altered and all points on the right side of the feature space are considered surge.

Using GPC, it could be possible to decrease the misclassification rate with use of a rejection zone. Such a region, called in this study a grey zone, can be understood as locations in feature space where no classification is made. It could be beneficial for avoiding false positive surge detection in the transition zone, where the probability for neither of the classes is high. Using GPC-modelled probabilities distribution, it is investigated if such approach would be viable and of practical use for compressor conditions classification using the available data.

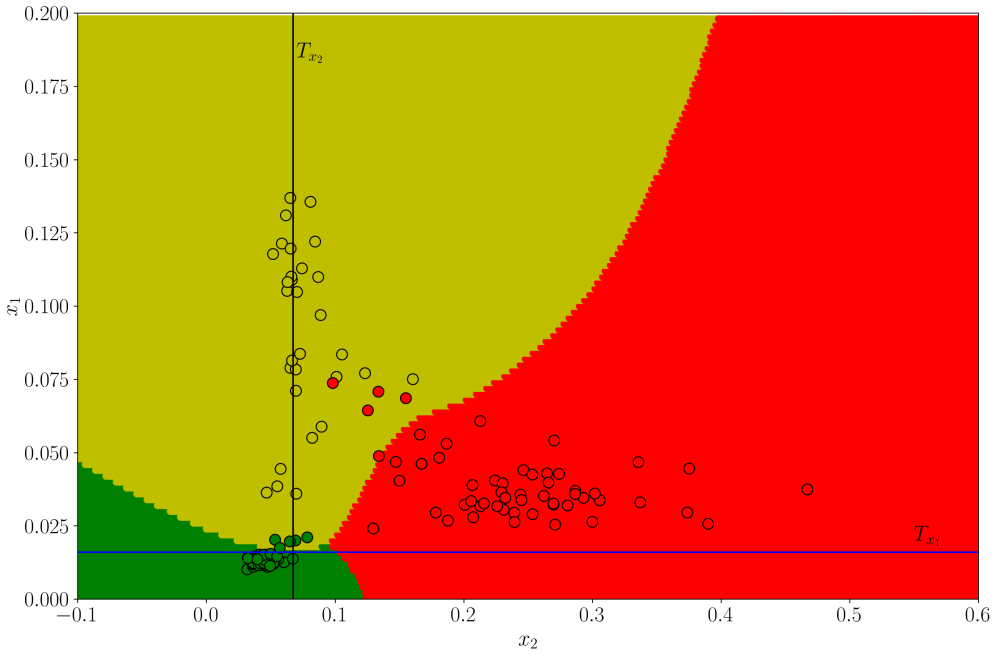

Figure 6: Class boundaries for GPC (colormap) and thresholds with reference to the test data (scatter points); green region marks the locations in the feature space which would be defined stable, yellow - inlet recirculation and red - surge; the class assignment was based on the highest probability value for a given location

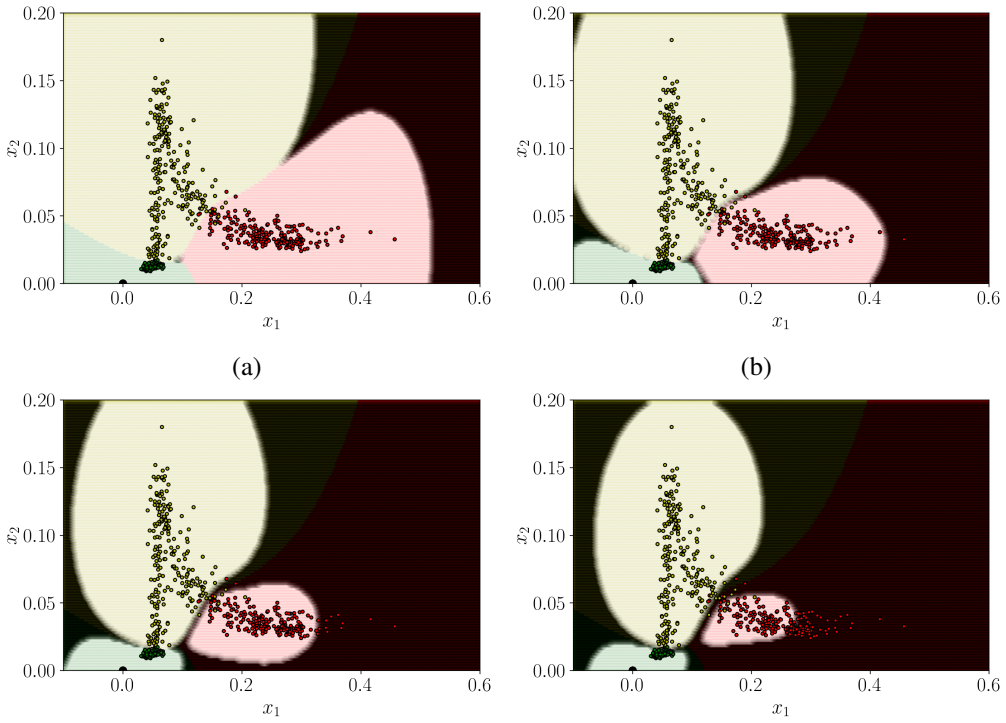

Figure 7: Grey zones for different probability limits a) 0.4, b) 0.5, c) 0.6, d) 0.7; dark regions indicate the grey zone, where the maximum value of any class probability is no higher than the limit; with rejection condition, no class would not be assigned in that region

In default classification approach, the highest probability value decides about the class assignment [18]. For

a binary case it is above 0.5, while for three classes it is above 0.(3). To investigate the grey zone potential, four threshold values of probability are chosen, being 0.4, 0.5, 0.6 and 0.7. Figure 7 shows grey zones for different levels of probability. For the lowest probability threshold, grey zone would first appear far away from the regions where data points are present. Increasing the probability limit, the grey zone becomes more and more present in between the classes, starting from the locations with low density of the training data, but also extends importantly in the regions far away from the transition zone. For the probability threshold of 0.6 or 0.7, the grey zone limits the size of the classes, in particular the surge class. In case of quick change in throttling, a quick transition to high x_2 value could be possible. Therefore, the first unstable point after stable conditions would lie far from from the threshold, but could land in grey zone and not be classified. This might lead to rejection of classification of the points for strong surge conditions, which should definitely be avoided in surge detection system.

To quantify the performance of GPC and compare it with the threshold approach, the effects of the test set classification are investigated. Figure 8 demonstrates the probability values for classes obtained from GPC and class assignment with threshold-based approach. The true class based on initial labels is also shown with the background shadow. The comparison focuses on the transition between inlet recirculation and surge as it was shown to be the most challenging for the threshold approach.

The results for inlet recirculation (Figure 8 a)) show that this instability is first detected for the same sample number with both methods. The indication for GPC remains relatively constant throughout the recirculation region, being close to value 1. This is consistent with what was observed in probability contours in Figure 5. For the threshold approach, several changes in predicted class are observed in the recirculation zone, which comes from the points being shifted slightly to the right side of the threshold. For surge indication, the GPC predictions are in line with the class labels. Assuming a default probability limit for classification, the indication of surge is consistent and no misclassifications are observed. The probability value of surge class is between 0.6 to 0.8 for most of the region, which is lower than what can be observed for inlet recirculation. The fluctuations of probability are also quite important. With the threshold approach, a number of false positive indications is observed between samples 60 and 80. This is complementary to misclassification in inlet recirculation zone. After the sample 75, which is roughly ten samples before data labelled as surge, the threshold indication of surge remains for the rest of the test data.

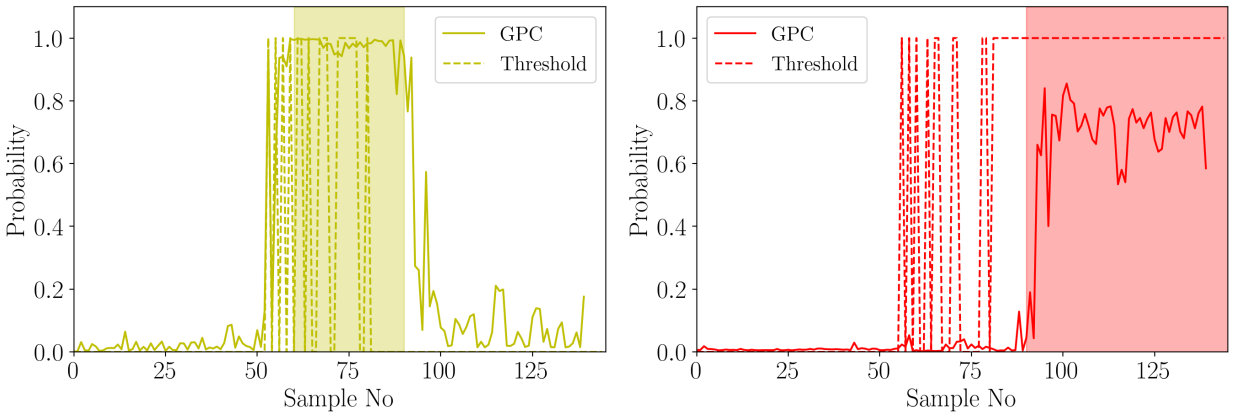

(a) (b)

Figure 8: Comparison of class probability and threshold classification for different instabilities a) inlet recirculation b) surge; shading in the background indicates the true class label that should be detected

Figure 9 depicts correct and incorrect classifications in the region of transition between inlet recirculation and surge classes. To better understand the location of misclassifications and investigate possible advantage of grey zone, the points belonging to grey zone for probability limit of 0.7 are marked with a red color for GPC plot. It can be seen that a few of the test set points fall within the grey zone. They are not located exactly in the transition zone, but rather at the beginning of the surge region, where the class probability is fluctuating. Therefore, using the test set it can be stated that the introduction of grey zone does not help

to avoid false positive surge indication in the transition region. The gray zone shape and influence would probably change if the data for two classes was not located so closely in the feature space.

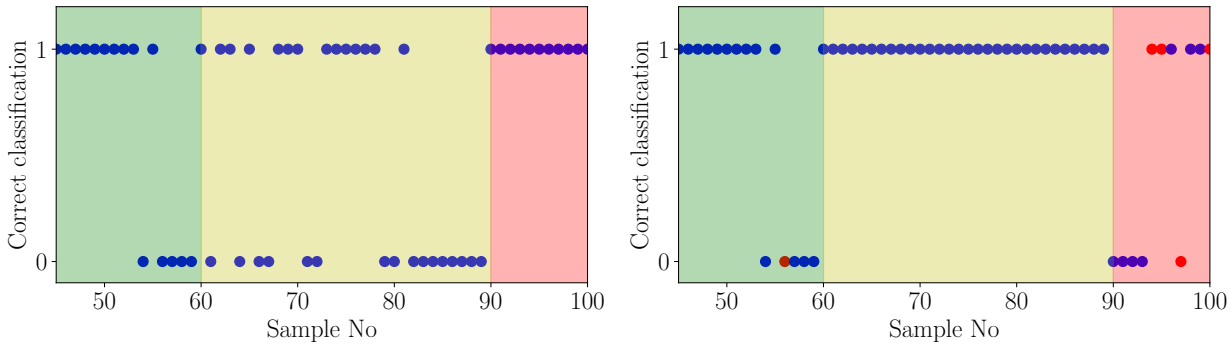

Figure 9: Correct and incorrect classification for a) threshold aproach and b) GPC approach; the background color indicates a true class for the data point, with green region being stable, yellow being inlet recirculation and red being surge, red points indicate the data points falling in the grey zone at probability limit 0.7

The threshold approach implemented based on stable conditions prove to be more conservative than the boundaries created using GPC. When considering data-driven boundaries, surge boundary is at much higher x_2 value than for threshold approach. As much as it can increase the operating range of the compressor, it should be thoroughly investigated if such placement is not dangerous for machine operation. The location of class boundary boundary with GPC will strongly depend on the training data labels, therefore those labels should be thoroughly checked. For the training dataset a single class label was assigned for each TOA value. As was presented in the previous study, with increasing throttling, the number of points from IR class that are classified as surge increases [12]. This might suggest that the fluid flow in the compressor might be temporarily unstable even for IR labelled points, making the global labelling misleading. If shorter portions of the input signal are considered, a label for each portion should be assigned and one should make sure it is correct. For a maximum extension of the operating range, the effects of given flow conditions on the structure should be investigated to understand the safety limits with respect to the features used for classification.

The GPC can provide a much better shaping of the thresholds between classes, very well adjusted to the training data. A much better accuracy of classification can be obtained compared to the threshold method. This increased accuracy comes at a price of needing to knowing all of the classes, which may be challenging for compressor operating at high pressure ratios. Overall, the application of advanced clustering technique is helpful in reaching better classification of the conditions.

When the whole operating range of the compressor is quantified and the data is properly labelled, the use of advanced classifier can be beneficial for the accuracy of detection. However, the advantage of the classification approach with use of GPC are the most important at transition between the classes. Further away from the transition, the type of kernel function and its hyperparameters have an important influence on the shape of probability distribution. With interpretable features used in this study, the increase in value of the feature can be associated with the increase of instability severity. Therefore, the combination of advanced classifier and feature interpretation could be proposed. The advanced classifier could be applied in the transition zone, where a flexible boundary shape is best suited to represent the data. The interpretation of features could be used away from the boundary. It would ensure that the points with high feature values, classification of which is easy with expert knowledge, did not get misclassified due to the classifier formulation.

5 Conclusions

In this study, the approach for classification of instabilities enhanced with a probabilistic method was investigated. The procedure involved transformation of the input signal trough empirical mode decomposition

to obtain a feature space representation of the conditions, following the method presented in a previous study [12]. Using a set of training data for a centrifugal compressor, the feature space was divided into three classes for stable, inlet recirculation and surge conditions observed in the machine. Two different approaches to classification were used, one with thresholds build based on a stable class feature values and the other, probabilistic, employing Gaussian process classification and using data for all of the classes. The methods were validated using a test dataset, representing dynamic transition from stable to unstable conditions. A special focus was on transition zone from inlet recirculation to surge, as it was shown to be the most challenging region to classify.

The application of GPC allowed to increase the accuracy of classification in the transition zone compared to the threshold method. The boundaries created with probabilistic classifier were capable of representing well the training data and output high accuracy of classification for the test data. Several misclassification were avoided in the transition zone. The output of GPC is driven by the input data and kernel function. The shape of the posterior distribution can be very case specific and changes to the input data or hyperparameters can drive the algorithm towards different solutions. Due to this, the certainty in labelling of the conditions for training is of a paramount importance. As for a given throttling level the stability can differ in time, the labelling method should be of sufficient granularity to capture this changes. For this reason, the procedure where one stability indication is given for a specific throttling could be reevaluated.

The probabilistic formulation of GPC offers a possibility to reject classification in some regions of feature space where the probability for each of the classes is low. The effects of rejection option did not seem to have important effect on the accuracy of classification. For closely spaced data in transition zone, the rejection condition was only present in the transition zone if the rejection threshold was high. For such a high threshold, the rejection zone was severely limiting the size of classes further away from the boundary, where the conditions are well understood due to interpretability of the features. Therefore, taking advantage of GPC in the transition zone and features interpretability further from this region could be the best approach for a robust classification, providing flexible, data-drive threshold and no misclassification problem further from the boundaries.

Overall, the application of GPC can allow to avoid too early surge detection and increase the operating range of the compressor compared to the threshold approach. This increase comes at a cost of having also the measurements for unstable conditions, which might be difficult to obtain. However, with increasing level of fidelity in computational models of compressors, synthetic data could be used for representing the unstable condition without the risk of machine destruction in the process. Further research is needed, but the approach proposed in this study can be a reliable and precise solution for a compressor monitoring system.

References

[1] H. P. Bloch, *A practical guide to compressor technology*. John Wiley & Sons, 2006.

[2] C. Schreiber, "Inlet Recirculation in Radial Compressors," Ph.D. dissertation, University of Cambridge, 2017.

[3] A. Bianchini, G. Andreini, L. Ferrari, D. T. Rubino, and G. Ferrara, "Development of a criterion for a robust identification of diffuser rotating stall onset in industrial centrifugal compressors," *Journal of Engineering for Gas Turbines and Power*, vol. 141, no. 2, 2019.

[4] R. Van den Braembussche, *Design and analysis of centrifugal compressors*. John Wiley & Sons, 2019.

[5] X. He and X. Zheng, "Flow instability evolution in high pressure ratio centrifugal compressor with vaned diffuser," *Experimental Thermal and Fluid Science*, vol. 98, pp. 719–730, 2018.

[6] W. C. Oakes, P. B. Lawless, J. R. Fagan, and S. Fleeter, "High-speed centrifugal compressor surge initiation characterization," *Journal of propulsion and power*, vol. 18, no. 5, pp. 1012–1018, 2002.

[7] M. Stajuda, G. Liskiewicz, and D. Garcia, "Flow Instabilities Detection in Centrifugal Blower Using Empirical Mode Decomposition," 2019.

[8] Y. Liu, K. Ma, H. He, and K. Gao, "Obtaining information about operation of centrifugal compressor from pressure by combining eemd and imfe," *Entropy*, vol. 22, no. 4, p. 424, 2020.

[9] A. Logan, D. G. Cava, and G. Liśkiewicz, "Singular spectrum analysis as a tool for early detection of centrifugal compressor flow instability," *Measurement*, p. 108536, 2020.

[10] M. Stajuda, D. García Cava, and G. Liśkiewicz, "Comparison of empirical mode decomposition and singular spectrum analysis for quick and robust detection of aerodynamic instabilities in centrifugal compressors," *Sensors*, vol. 22, no. 5, p. 2063, 2022.

[11] B. D. Fulcher, "Feature-based time-series analysis," in *Feature engineering for machine learning and data analytics*. CRC Press, 2018, pp. 87–116.

[12] M. Stajuda, D. G. Cava, and G. Liśkiewicz, "Aerodynamic instabilities detection via empirical mode decomposition in centrifugal compressors," *Measurement*, p. 111496, 2022.

[13] C. K. Williams and C. E. Rasmussen, *Gaussian processes for machine learning*. MIT press Cambridge, MA, 2006, vol. 2, no. 3.

[14] N. E. Huang, *Hilbert Huang Transform and its applications*. World Scientific, 2014.

[15] C. M. Bishop and N. M. Nasrabadi, *Pattern recognition and machine learning*. Springer, 2006, vol. 4, no. 4.

[16] D. Duvenaud, "The kernel cookbook: Advice on covariance functions," *URL https://www. cs. toronto. edu/˜ duvenaud/cookbook*, 2014.

[17] K. P. Murphy, *Machine learning: a probabilistic perspective*. MIT press, 2012.

[18] F. Pedregosa, G. Varoquaux, A. Gramfort, V. Michel, B. Thirion, O. Grisel, M. Blondel, P. Prettenhofer, R. Weiss, V. Dubourg, J. Vanderplas, A. Passos, D. Cournapeau, M. Brucher, M. Perrot, and E. Duchesnay, "Scikit-learn: Machine learning in Python," *Journal of Machine Learning Research*, vol. 12, pp. 2825–2830, 2011.

[19] K. Botros and J. Henderson, "Developments in centrifugal compressor surge control—a technology assessment," 1994.

[20] G. Liśkiewicz, L. Horodko, M. Stickland, and W. Kryłłowicz, "Identification of phenomena preceding blower surge by means of pressure spectral maps," *Experimental Thermal and Fluid Science*, vol. 54, pp. 267–278, 4 2014.